Application of the Stretched Exponential Function to Fluorescence Lifetime Imaging

K. C. Benny Lee,* J. Siegel,* S. E. D. Webb,* S. Lévêque-Fort,* M. J. Cole,* R. Jones,* K. Dowling,* M. J. Lever,† and P. M. W. French*

*Department of Physics, Imperial College of Science, Technology, and Medicine, London SW7 2BW, and †Department of Biological and Medical Systems, Imperial College of Science, Technology, and Medicine, London SW7 2BY, United Kingdom

ABSTRACT Conventional analyses of fluorescence lifetime measurements resolve the fluorescence decay profile in terms of discrete exponential components with distinct lifetimes. In complex, heterogeneous biological samples such as tissue, multi-exponential decay functions can appear to provide a better fit to fluorescence decay data than the assumption of a mono-exponential decay, but the assumption of multiple discrete components is essentially arbitrary and is often erroneous. Moreover, interactions, both between fluorophores and with their environment, can result in complex fluorescence decay profiles that represent a continuous distribution of lifetimes. Such continuous distributions have been reported for tryptophan, which is one of the main fluorophores in tissue. This situation is better represented by the stretched-exponential function (StrEF). In this work, we have applied, for the first time to our knowledge, the StrEF to time-domain whole-field fluorescence lifetime imaging (FLIM), yielding both excellent tissue contrast and goodness of fit using data from rat tissue. We note that for many biological samples for which there is no a priori knowledge of multiple discrete exponential fluorescence decay profiles, the StrEF is likely to provide a truer representation of the underlying fluorescence dynamics. Furthermore, fitting to a StrEF significantly decreases the required processing time, compared with a multi-exponential component fit and typically provides improved contrast and signal/noise in the resulting FLIM images. In addition, the stretched-exponential decay model can provide a direct measure of the heterogeneity of the sample, and the resulting heterogeneity map can reveal subtle tissue differences that other models fail to show.

INTRODUCTION

Fluorescence lifetime imaging is based on the measurement of the decay in fluorescence intensity across a sample after optical excitation. Functional information may be derived from fluorescence lifetime via its dependence on fluorophore radiative and non-radiative decay rates. It may be used to distinguish between different fluorophore molecules (with different radiative decay rates) or to monitor local environmental perturbations that affect the non-radiative decay rate. This functionality has been exploited to quantify physiological parameters including pH (Sanders et al., 1995; Szmacinski and Lakowicz, 1993), $[Ca^{2+}]$ (Lakowicz et al., 1992), and pO_2 (Bambot et al., 1995). Because fluorescence lifetime is derived from relative intensity values, it can provide useful information concerning biological tissue despite the heterogeneity and strong optical scattering. Fluorescence lifetime imaging (FLIM), in which a map of the spatial distribution of fluorophore lifetimes is displayed, thus provides a powerful functional imaging modality for biomedicine. One promising application is to study protein structure and function, utilizing the sensitivity of their endogenous fluorescence to the physiochemical properties of the environment.

Received for publication 15 September 2000 and in final form 23 May 2001.

Address reprint requests to Dr. Jan Siegel, Imperial College of Science, Technology, and Medicine, Femtosecond Optics Group, The Blackett Laboratory, Prince Consort Road, London SW7 2BW, UK. Tel.: 44-20-7594-7788; Fax: 44-20-7594-7782; E-mail: j.siegel@ic.ac.uk.

0006-3495/01/09/1265/10 $2.00

In practice, FLIM can be realized either in the frequency domain or the time domain. In principle, time-resolved and frequency-resolved data are equivalent and are related via the Fourier transform (Clegg and Schneider, 1996). Frequency-domain FLIM can be more straightforward to implement experimentally and is more light efficient. However, it suffers from a limited temporal dynamic range and the analysis of complex exponential decays can become rather intractable. Time-domain FLIM requires ultra-fast laser technology but is often better suited to studying complex exponential decays, particularly when the various lifetime components are very different. The recent development of ultra-fast laser and imaging technology enables the demonstration of potentially inexpensive time-domain FLIM instruments (Jones et al., 1999).

In our laboratory, time-domain FLIM data are obtained by acquiring a series of time-gated fluorescence intensity maps at increasing delays after excitation by ultra-short laser pulses. The temporal series of relative fluorescence intensity values for each pixel in the field of view can then be fitted to an assumed decay model, conventionally a multiple-exponential function with discrete lifetimes.

In general, we have observed that the autofluorescence decays of collagen, elastin, and other tissue components do not fit a single-exponential decay profile and that the assumption of a double-exponential decay provides a better fit (Dowling et al., 1998). However, an apparently satisfactory fit to such a model, e.g., a double-exponential model, can conceal the actual complexity in the decay mechanisms (James and Ware, 1985). There are many situations in

which one does not expect a limited number of discrete decay times; e.g., for a fluorophore in a mixture of solvents, such that a range of fluorophore environments exists, each environment results in a different intensity decay (Lakowicz, 1999). For a single-tryptophan protein, for instance, the resulting distribution of protein conformations may lead to a continuous distribution of fluorescence lifetimes (Alcala et al., 1987; Alcala, 1994). Another possibility is a protein that has so many tryptophan residues that it is not practical to consider the individual decay times (Lakowicz, 1999). Generally, these variations are present on a molecular scale and therefore cannot be spatially resolved. In these cases, fitting to a double-exponential model would imply an erroneous assumption of two discrete lifetimes. Although it would provide a better fit than the single-exponential, due to the extra two fitting parameters, its use cannot be justified from a physical point of view. Similarly, triple- or higher-exponential decay models will improve the goodness of fit solely by the extra fitting parameters and not due to a better description of the experimental decay dynamics. Thus, the choice of the number of exponential decay terms is arbitrary if justified only by the goodness of fit.

In this work the stretched-exponential function (StrEF) is proposed as an alternative model to fit the fluorescence decay of complex samples, in particular, biological tissue, studied by fluorescence lifetime imaging. Also known as the Kohlrausch-Williams-Watts function, the StrEF was first studied by Kohlrausch in 1847 as an empirical description for the structural relaxation of glassy fibers and subsequently used by G. Williams and D. C. Watts to describe dielectric relaxation in polymers. Since then, a large number of relaxation systems (ranging from earthquakes, galactic light emissions, and biological extinction to economics and scientific citations) have been found to exhibit this type of function (Laherrère and Sornette, 1998), and numerous underlying physical mechanisms have been proposed for their derivations (Phillips, 1996).

Our motivation to apply the StrEF to FLIM of biological tissue is that, from a mathematical point of view, the stretched-exponential decay can be expressed as a continuous distribution of lifetimes (Alvarez et al., 1991). This model should therefore be more appropriate to describe the decay in heterogeneous tissue samples showing continuous lifetime distributions than multi-exponential models with an arbitrary number of discrete lifetimes. In particular, continuous distributions of the fluorescence lifetime have been reported for proteins such as tryptophan, which are considered the major fluorophores in biological tissue when excited in the UV (Alcala et al., 1987). We have applied the StrEF to whole-field FLIM and demonstrate that this decay model yields strong contrast in tissue discrimination, without compromising the goodness of fit. In addition, unlike other models, the StrEF provides a direct measure of the local heterogeneity of the sample, which is related to the width of the lifetime distribution.

In the following sections some mathematical ideas related to the application of the stretched-exponential function in FLIM are introduced and the implementation of this model to whole-field FLIM images is presented.

THEORETICAL BACKGROUND

After optical excitation, an excited singlet electron in a fluorophore molecule will return to its ground state with the emission of a photon, giving rise to fluorescence. Under the typical assumption of a non-interacting environment, the fluorescence decay rate is written as:

$$\frac{dN}{dt} = -CN, \tag{1}$$

where N is the number of excited electrons and C is the decay constant. Solving Eq. 1 will yield the conventional single-exponential decay function.

However, the presence of progressively depleted random sinks that capture excitations (Phillips, 1996) can modify a spontaneous decay process represented by Eq. 1, such that the decay rate itself is dependent on time, stretching the decay:

$$\frac{dN}{dt} = -C\frac{N}{t^{\gamma}}, \tag{2}$$

where γ is a characteristic constant. Assuming that the fluorescence intensity is proportional to the decay rate, Eq. 2 then leads to the stretched-exponential function given by:

$$I(t) = I_0 \exp\left[-\left(\frac{t}{\tau_{\mathrm{kww}}}\right)^{1/\mathrm{h}}\right], \tag{3}$$

where $I(t)$ is the fluorescence intensity at time t, I_0 is the fluorescence intensity at time 0, τ_{kww} is the characteristic time scale of the decay and h (≥ 1) is the heterogeneity parameter of the sample ($h = 1 \rightarrow$ homogeneous). τ_{kww}, h, C, and γ are related such that $h = 1/(1 - \gamma)$ and $(\tau_{\mathrm{kww}})^{1-\gamma} = (1 - \gamma)/C$.

The presence of progressively depleting random sinks in fluorescence has previously been encountered in fluorescence resonance energy transfer (FRET). Theodor Förster predicted in 1948 that the fluorescence intensity decay of a donor molecule in the presence of FRET obeys a stretched-exponential law (Förster, 1948). The heterogeneity parameter h was expected to have discrete values (2, 3, and 6) dependent on the dimension of the system, which has been verified experimentally by several groups, e.g., Maliwal et al. (1994), who studied a one-dimensional system composed of fluorophores bound to a linear DNA double helix (Maliwal et al., 1994). This demonstrates the validity of a stretched-exponential decay in FRET, and it should in principle be straightforward to establish its validity in FLIM of biological tissue due to energy transfer and energy migra-

tion mechanisms occurring in tissue (Ghiggino and Smith, 1993). Nevertheless, it is also important to realize that the scenario mentioned before, i.e., a spatially unresolvable single-tryptophan protein in a range of different microenvironments and/or a protein with many tryptophan residues, directly leads to a stretched-exponential decay, even in the absence of energy transfer mechanisms. This is so because such a scenario yields a continuous distribution of lifetimes and the stretched exponential function in Eq. 3 can be mathematically expressed as a superposition of exponential terms as follows:

$$I(t) = \int_0^\infty \exp\left(-\frac{t}{\tau}\right)\rho(\tau)d\tau, \tag{4}$$

where $\rho(\tau)$ is the continuous distribution of lifetimes. Because such continuous lifetime distributions due to a range of microenvironments, either from a variation in the number of adjacent solvent molecules and/or from different protein conformations, have been observed for tryptophan (Alcala et al., 1987; Alcala, 1994), the mathematical equivalence of Eqs. 3 and 4 predicts a stretched-exponential decay of the autofluorescence in biological tissue.

SIMULATIONS

The mathematical equivalence between the StrEF (Eq. 3) and the expression for the continuous lifetime distribution (Eq. 4) was tested by way of a simulation. Sets of data that included an element of Poisson noise were simulated using:

$$I = \sum_{j=1}^{J} \alpha_j \exp\left(-\frac{t}{\tau_j}\right) + Poisson\ noise, \tag{5}$$

where τ_j values are lifetimes chosen to emulate experimental values, α_j values are the fractional contribution of each of these components, and J determines the total number of exponential terms used for simulating a particular set of data. Fig. 1 *a* illustrates the degree to which the stretched-exponential function fits simulated multiple-exponential decay profiles. We have studied the influence of relative intensities of individual components by using a decay profile where all but the longest lifetime component are of equal intensity. This is done by introducing a factor R, defined as:

$$R(J) = \frac{\alpha_J}{\alpha_{<J}}, \tag{6}$$

with $\alpha_{<J} = \alpha_1, \alpha_2, \ldots \alpha_{J-1}$ and with $R(1) = 1$. A larger R indicates that the longer lifetime dominates in the data set. The figure of merit (goodness of fit) used was the statistical χ^2/(degrees of freedom), defined as:

$$\frac{\chi^2}{dof} = \frac{1}{N-m}\sum_{i-1}^{N}\frac{[I_i - I(t_i)]^2}{\sigma_i^2}, \tag{7}$$

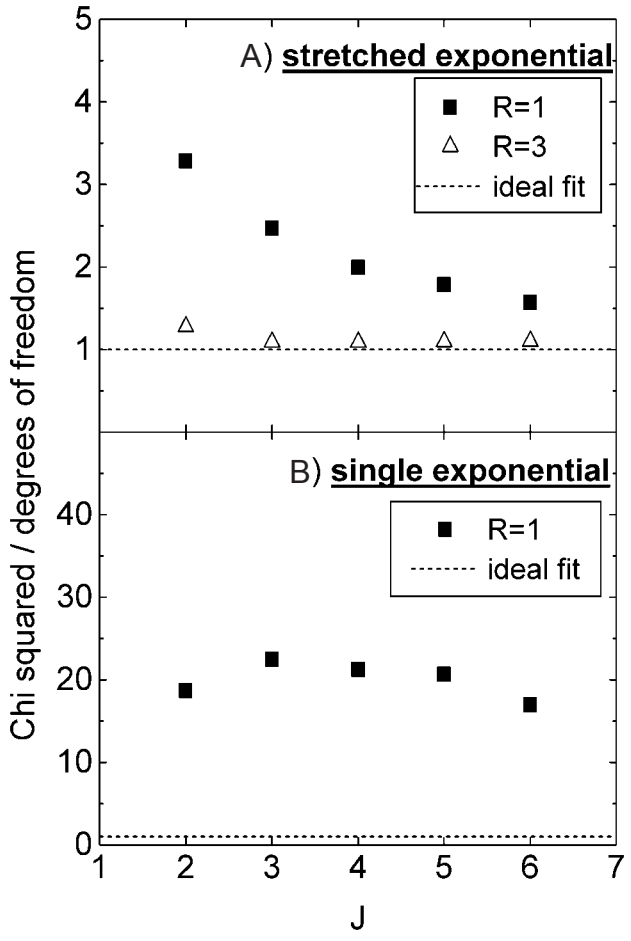

FIGURE 1 Performance of the stretched exponential function (*A*) and the single-exponential function (*B*) in describing multi-exponential decay data.

where t_i, I_i values are the pairs of N data points, σ_i values are the expected standard deviation of the data points, and m is the number of fitting parameters. An ideal fitting model will be indicated by a value of one for χ^2/(degrees of freedom (*dof*)).

It can be seen from Fig. 1 *a* that the stretched-exponential function becomes a better fitting model as the number of exponential terms increases, approaching ideality as the number tends to infinity. (An exception exists when only one exponential term is used for the simulation, in which case the stretched exponential model fits the simulated data ideally with $h = 1$.) This confirms the mathematical equivalence between the StrEF (Eq. 3) and the expression for the continuous lifetime distribution (Eq. 4). It can also be seen that the data fitting approaches ideality as R increases because an increased dominance of one lifetime component over the other(s) is similar to a StrEF with a small heterogeneity parameter. From a practical point of view, this is important because it implies that the StrEF can even be applied to fluorophores where a multi-exponential decay

with one dominant component has been demonstrated to occur, without compromising the goodness of fit significantly.

To get a more quantitative impression of the goodness of fit when using a StrEF to fit multi-exponential data, one of the sets of data ($R = 1$, i.e., equal relative intensities of the lifetime components) was also fitted to a single-exponential function, and this is shown in Fig. 1 *b*. It can be seen that all single-exponential fits to multiple-exponential data were equally unreliable ($\chi^2/dof \approx 20$), independent of J. For the same set of data ($R = 1$), the stretched-exponential model yields a considerably better goodness of fit even for the case of its worst performance: the double-exponential decay ($\chi^2/dof < 3.5$). Also here, from a practical point of view, an important conclusion can be drawn because a single-exponential model is commonly used in FLIM as a first guess due to the short calculation time. The comparison of Fig. 1, *a* and *b*, suggests that the use of the StrEF provides a dramatically better fit to multi-exponential decays than a single-exponential fit without an excessive increase in calculation time (only a factor of ~1.5). It is worth noting that even in the case of a purely single-exponential decay, the StrEF gives the correct result because this corresponds to its degenerate form with $h = 1$.

So far, we have considered the performance of the StrEF on simulated decay data that are purely multi-exponential. Experimental fluorescence decay profiles, however, are often not multi-exponential decays. As pointed out before, a multi-exponential model neglects the interaction between fluorophores and their environment in complex samples such as biological tissue, which yields continuous distributions rather than a few discrete lifetimes. In the following we have studied the performance of the StrEF in fitting real whole-field FLIM data of rat tissue.

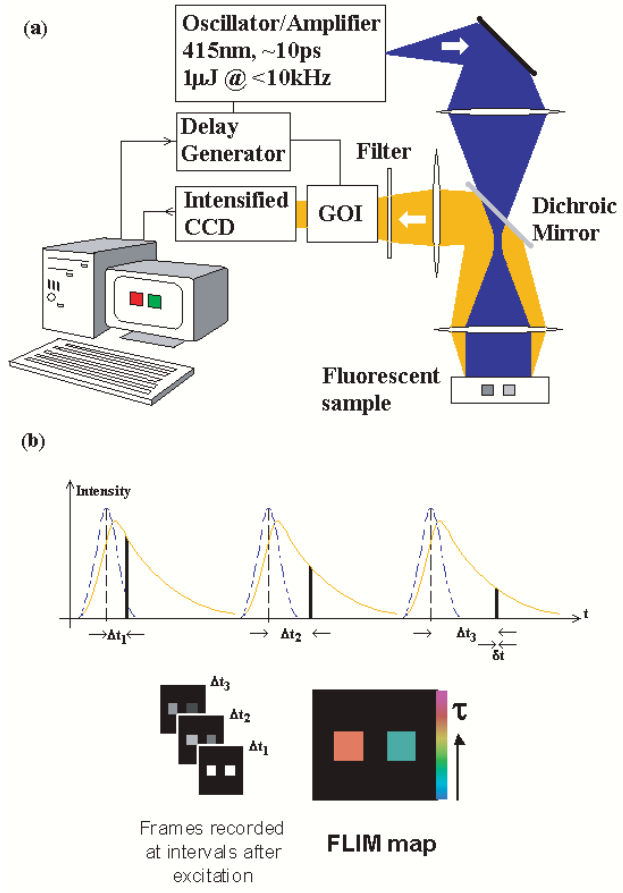

FIGURE 2 (*a*) Schematic of the experimental FLIM system; (*b*) The acquisition process.

METHODS

Our time-domain FLIM apparatus and the data acquisition schema are shown in Fig. 2. The excitation source is a commercial ultra-fast Ti:sapphire laser oscillator (Tsunami, Spectra Physics, Herts, U.K.), the output of which is amplified in a home-built Cr:LiSAF regenerative amplifier pumped by the same argon-ion laser as the oscillator. This produces pulses of ~ 0-μJ energy and 10-ps duration at a 5-kHz repetition rate at ~830 nm. These pulses are then frequency doubled to produce a 1-μJ whole-field excitation source at 415 nm for the tissue sample. The spatial intensity distribution of the tissue autofluorescence is imaged onto a gated optical intensifier (Kentech Instruments, Didcot, U.K.), which acquires whole-field two-dimensional intensity images with an effective gate width of ~90 ps, including timing jitter. FLIM maps are produced by acquiring a series of time-gated fluorescence intensity images at a range of time delays after excitation and, for each pixel in the field of view, fitting the assumed decay profile using the Marquardt algorithm for nonlinear least-squares fits (Bevington, 1969). When applied to simple fluorophore distributions, this instrument can provide FLIM maps with an update time of only 3 s (Dowling et al., 1999) and resolve lifetime differences of <10 ps (Dowling et al., 1998).

In this work we compare FLIM maps obtained using single-, double-, and stretched-exponential fits. In the case of the single-exponential fit, the lifetime τ is used as the plotting parameter on a pseudo-color map for display. In the case of the double-exponential fit, the short (τ_1) and the long (τ_2) lifetime components are used, together with their weighted average value τ_{av}. In the case of the stretched-exponential function, it is necessary to interpret the lifetimes in a statistical manner to correctly describe a decay given by Eqs. 3 and 4. One possibility of such a statistical interpretation of the continuous lifetime distribution is the 95th-percentile lifetime (Laherrère and Sornette, 1998). We have chosen to work with the mean lifetime of the distribution that is directly obtained from the integration of Eq. 3, given by:

$$\langle \tau \rangle = h\tau_{kww}\Gamma[h], \tag{8}$$

where $\Gamma[z]$ is the gamma function. Unlike multi-exponential models, the StrEF offers an additional parameter of potential interest: the heterogeneity parameter h. This parameter is related to the stretching of the decay process and a direct measure of the width of the lifetime distribution. In addition to the mean lifetime $\langle \tau \rangle$ as a plotting parameter, we have therefore also plotted h on a grayscale map.

RESULTS

The autofluorescence of individual components can be used to contrast different types of biological tissue or different states of tissue. This can provide a powerful diagnostic tool,

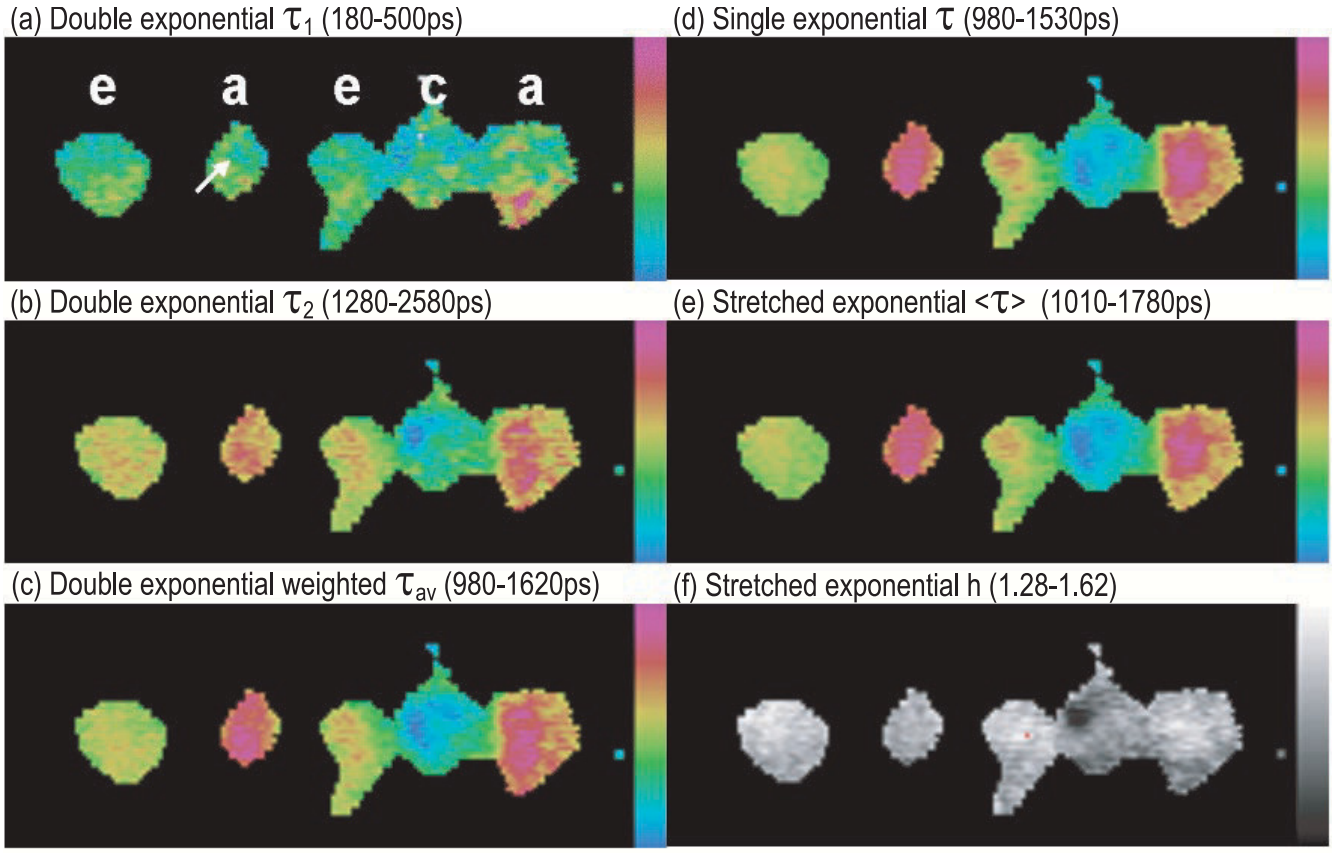

FIGURE 3 FLIM maps of aorta (a), collagen (c), and elastin (e). (*a–c*) Short-lived (*a*) and long-lived (*b*) lifetime components, and their weighted average for the double-exponential model (*c*); (*d*) Lifetime for the single-exponential model; (*e* and *f*) Mean lifetime (*e*) and heterogeneity parameter (*f*) for the stretched exponential model. The lifetime false color scale and the heterogeneity gray scale span over the range given in each individual map, where blue (black) represents low lifetime (heterogeneity) values and pink (white) high lifetime (heterogeneity) values. The arrow in *a* indicates the coordinates of the single pixel analysis shown in Fig. 4.

but unfortunately, conventional fluorescence intensity imaging and even fluorescence spectroscopy often fail to distinguish many tissue constituents. In some cases, however, FLIM can provide the desired contrast. We have previously applied FLIM to tissue components, such as collagen and elastin, which are considered the major fluorophores for excitation at 415 nm, whereas tryptophan and NADH dominate when excited in the UV (Baraga et al., 1991). The fluorescence observed for this excitation wavelength is attributed to the cross-linkages in collagen and elastin (Pongor et al., 1984). Like single-tryptophan proteins (Alcala et al., 1987), we also expect elastin and collagen to show continuous lifetime distributions rather than a few discrete lifetimes due to a range of microenvironments.

All components were extracted from rat, and the elastin was obtained by hydrolyzing aorta. For excitation at 415 nm, collagen and elastin have similar fluorescence spectra, but they may be successfully contrasted using fluorescence lifetime (Dowling et al., 1998). However, the choice of the decay model (i.e., single-exponential or double-exponential decay) was found to impact the specificity of tissue discrimination and the quality of the FLIM maps. Fig. 3 shows FLIM maps of collagen, aorta, and elastin obtained by single-, double-, and stretched-exponential decay models. The lifetime ranges have been scaled to minimize any unnecessary cropping of the deduced lifetimes. In Fig. 3 *a*, the short-lived component (τ_1) of the double-exponential decay can be seen, which does not show any significant contrast between the different tissues. The longer-lived component (τ_2), although clearly distinguishing the collagen and elastin, shows only a slight difference in lifetime between elastin and aorta (Fig. 3 *b*). In both cases the FLIM maps are relatively noisy because the fluorescence decay is separated into two components, which reduces the signal/noise ratio of the individual components. To overcome this, we have calculated the weighted average value τ_{av} of both components (Fig. 3 *c*), which shows a clear contrast between the three different tissue constituents. Nevertheless, despite the good contrast obtained, we want to stress that this weighted average value τ_{av} has no physical meaning whatsoever and is merely a way to improve image quality. This is because it is derived from a double-exponential

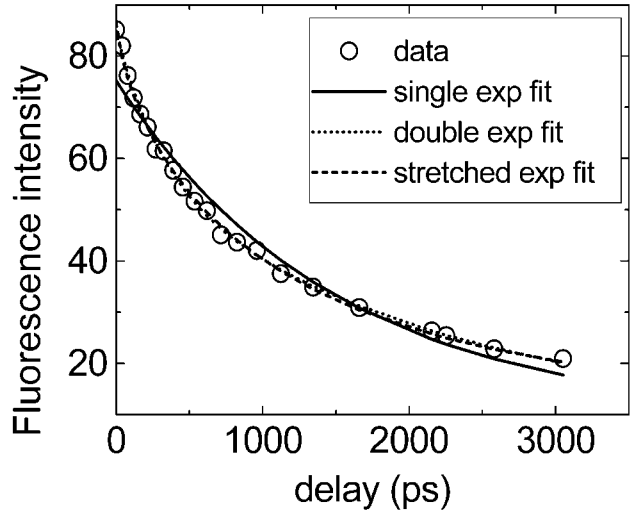

FIGURE 4 Single pixel analysis on the random aorta pixel indicated by an arrow in Fig. 3 upon application of various fitting models.

decay model assuming two discrete lifetime components as opposed to the continuous distributions of lifetimes usually present in biological tissue. Because the number of exponential terms chosen (two in this case) is arbitrary, a weighted average of two components would give a value somewhere in between these two components where no actual lifetime value can possibly lie in a double-exponential model. In this sense, the use of a single-exponential model would physically be at least as appropriate, providing a single lifetime value that approximately represents the center of the lifetime distribution for a significantly reduced calculation time. In Fig. 3 *d* it can be seen that a single-exponential fit provides as good contrast between the different tissue constituents as the weighted average value τ_{av} from the double-exponential fit.

Concerning the stretched-exponential fit, Fig. 3 *e* demonstrates that plotting the physically more representative mean value $\langle\tau\rangle$ of the continuous lifetime distribution $\rho(\tau)$ yields also provides strong contrast. In addition, the map of the heterogeneity parameter h (Fig. 3 *f*) shows a local inhomogeneity in the collagen where h has a very low value, corresponding to a narrower lifetime distribution than the surrounding area. Such additional detail revealed by the heterogeneity parameter may be useful in distinguishing local differences in protein conformations.

To further assess the different fitting models, we have plotted a typical data set for a single pixel in the field of view (indicated by an arrow in Fig. 3) together with the corresponding fitted curves (Fig. 4). We observe that the single-exponential model provides a poor fit to the data, despite the fact that it yields a FLIM map with good contrast. This means that the use of a single-exponential model yields incorrect absolute values of the lifetime data but is nonetheless sensitive to spatial variations in fluorescence lifetime. On the other hand, the double-exponential model provides a satisfyingly good fit to the data, but only the plotting of the physically meaningless parameter τ_{av} yields good contrast in the FLIM map. The stretched-exponential model, however, provides both a satisfyingly good fit to the data (Fig. 4) and good contrast when plotting the physically meaningful parameter $\langle\tau\rangle$ (Fig. 3 *e*). This suggests that the StrEF is the most appropriate model to distinguish different tissue constituents. The fact that the hydrolyzed elastin can be contrasted from the basic aorta is important as it suggests that we may be able to use FLIM as a means to provide a quantitative indication of the state of tissue, in particular, the state of the protein cross-linkages.

We have also applied the different decay models to whole-field FLIM data of unstained rat tissue sections. For comparison, Fig. 5 *a* shows a commercial light-microscope image of a stained tissue section from a rat's ear, highlighting two veins, an artery, cartilage, and some hair. A time-gated autofluorescence intensity image of a similar but unstained section, obtained using our home-built laboratory microscope, is shown in Fig. 5 *b*, and the corresponding FLIM maps are shown in Fig. 5, *c–h*. When fitting to a double-exponential decay, we again find that only by plotting τ_{av} (Fig. 5 *e*) can we obtain good contrast and spatial image quality. (Spatial image quality is a measure of lifetime variability between connected pixels within regions of the same average lifetime; image contrast measures lifetime variation between averaged regions.) The FLIM maps of the individual discrete components (Fig. 5, *c* and *d*) exhibit relatively poor contrast and spatial image quality due to the reduced signal/noise ratio. We wish to stress that although the maps of τ_{av} from the double-exponential decay fit do provide reasonable contrast and image quality, this parameter is physically meaningless and therefore cannot be used for quantitative analysis. On the other hand, the stretched-exponential function based on a continuous lifetime distribution does represent the likely physical origin of the observed fluorescence decay profiles, and the FLIM map of $\langle\tau\rangle$ from the StrEF (Fig. 5 *g*) also exhibits excellent contrast and spatial image quality. In addition, the StrEF provides additional information about the sample heterogeneity through the map of the parameter h (Fig. 5 *h*). For this tissue section, all the biological structures in the section exhibit a similar low heterogeneity value except the veins and arteries, which exhibit relatively high values. Because these vessels retained blood that had clotted postmortem, we believe that the high h values are characteristic of clotted blood. This significant difference in the h values between the blood-containing vessels and the surrounding tissue provides an even better image contrast than that obtained by plotting lifetime values. Thus, it becomes possible to identify other, much smaller regions of clotted blood, such as the one located to the right of the upper vein.

We note that the fluorescence lifetime map obtained using a single-exponential function (Fig. 5 *f*) shows contrast

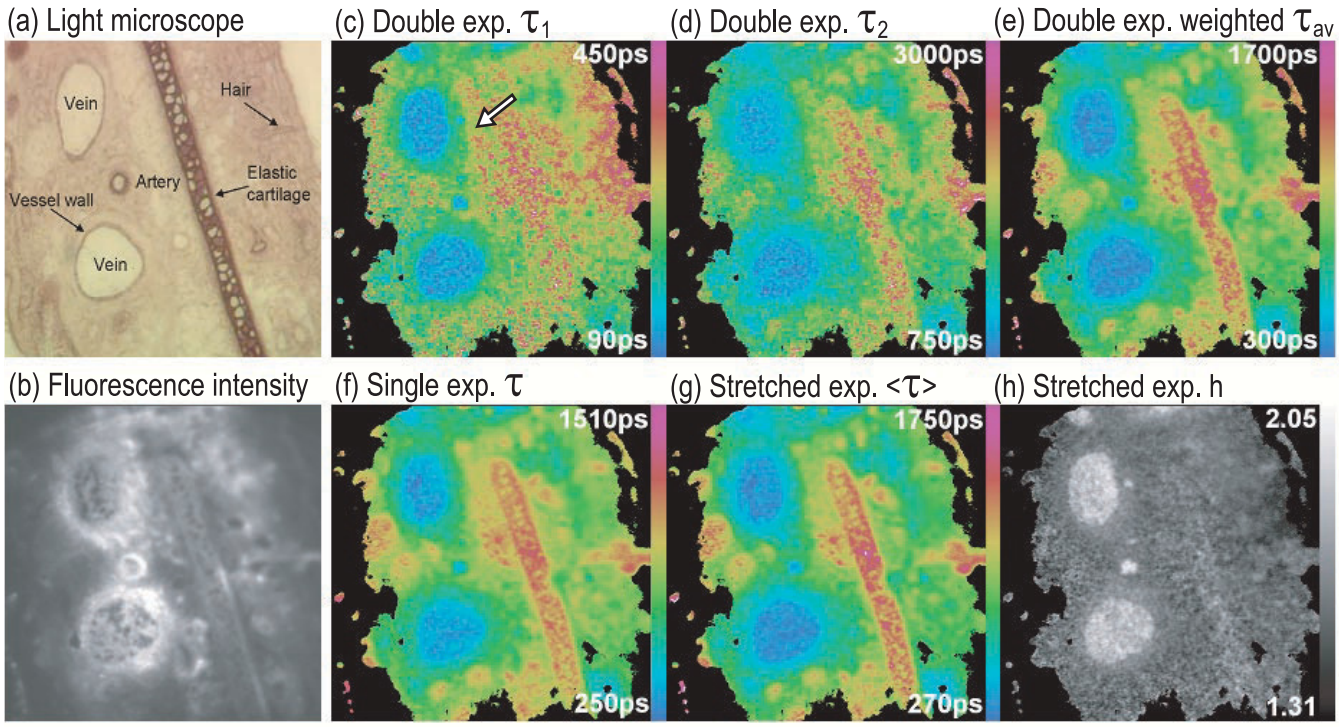

FIGURE 5 (*a*) Light microscope image of a stained tissue section from a rat's ear, highlighting the two veins, an artery, and elastic cartilage; (*b*) The time-gated fluorescence intensity image from a similar unstained tissue section as obtained with our FLIM apparatus; (*c–e*) The corresponding FLIM maps are shown for the short-lived (*c*) and the long-lived (*d*) lifetime components, and their weighted average for the double-exponential model (*e*); (*f*) The lifetime for the single-exponential model; (*g* and *h*) the mean lifetime (*g*) and the heterogeneity parameter (*h*) for the stretched-exponential model. The lifetime false color scale and the heterogeneity gray scale spans over the range given in each individual map. The arrow in *c* indicates the coordinates of the single pixel analysis shown in Fig. 6.

and spatial quality that are comparable to the lifetime map obtained with the stretched-exponential model (Fig. 5 *g*). However, analysis of the goodness of fit for the data from a typical pixel, as shown in Fig. 6, illustrates a much better fit for the stretched-exponential model, as evinced by the systematic drift of the residue and significantly higher χ^2/dof for the single-exponential function (as predicted by Fig. 1). This indicates that the single-exponential function is an incorrect choice for representing the fluorescence decay. Such an incorrect assumption can compromise the ability of FLIM maps to display subtle differences in experimental data, as illustrated in Fig. 7. Fitting to two distinct sets of data (which were simulated in this case) produced the same single-exponential decay curve and lifetime, even though the two sets of data are different. Fitting the stretched-exponential function to the same data sets, however, produced significantly different mean lifetimes of 910 ps and 940 ps for sets A and B, respectively.

DISCUSSION

The use of the stretched-exponential function for analyzing fluorescence decay profiles has been shown to provide excellent tissue discrimination and spatial image quality in whole-field FLIM maps. Even more importantly, the stretched-exponential function not only describes the decay profiles almost exactly but also derives from the more realistic decay model of continuous lifetime distributions in biological tissue, rather than from an arbitrary assumption of single or multiple discrete exponential decay components. This has the potential of revealing subtle differences in fluorescence decay profiles, possibly improving the specificity of FLIM. Moreover, this new approach yields, besides the mean lifetime $\langle\tau\rangle$ of the distribution, an additional parameter of interest (h), which is related to the width of the lifetime distribution and which is a direct measure for the local heterogeneity of the sample. The heterogeneity parameter is important because it enables the study of mechanisms that cause a continuous lifetime distribution to broaden or narrow. Future work on a variety of different tissue types and in different environmental conditions will hopefully provide more insight in this matter.

We note that there is ongoing discussion concerning whether proteins show distributions of lifetimes or discrete components. Vix and Lami (1995) report that the width of lifetime distributions of various single-tryptophan proteins is relatively small (a width of 1.4 ns full width at half-maximum with a center lifetime of 7 ns, for instance). For

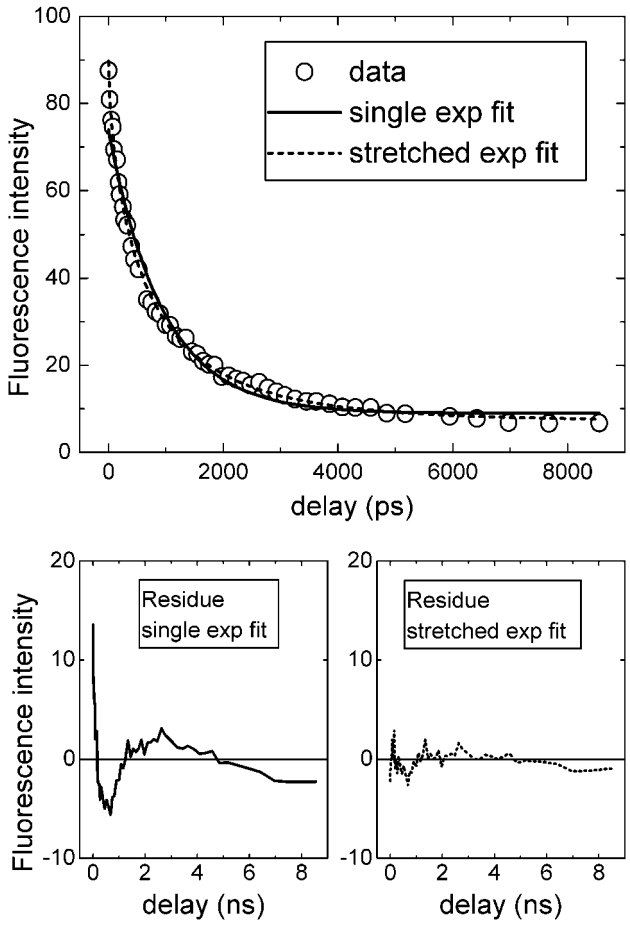

FIGURE 6 Single pixel analysis on the random pixel indicated by an arrow in Fig. 5 (rat's ear image). χ^2/dof (single) = 11.9; χ^2/dof (stretched) = 1.1

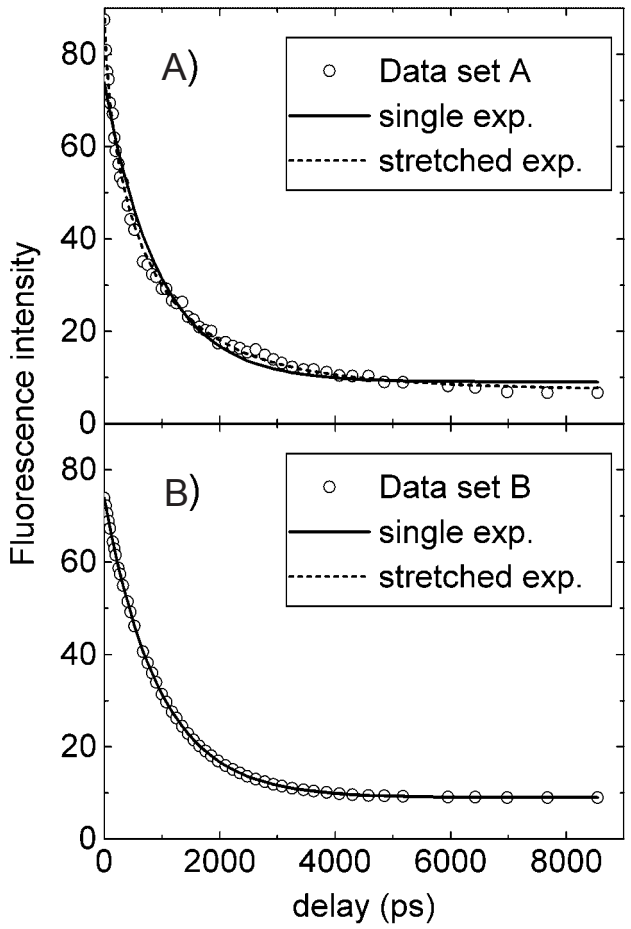

FIGURE 7 Performance of single- and stretched-exponential fits on distinct data sets. (*A*) Data set A, lifetime deduced by a single-exponential fit = 940 ps, by a stretched-exponential fit = 910 ps; (*B*) Data set B, lifetime deduced by a single-exponential fit = 940 ps, by a stretched-exponential fit = 940 ps.

this reason they favor discrete components over distributions, as opposed to other authors (e.g., Alcala, 1994) who work with continuous distributions. Even if one considers such a width/center ratio small enough to be negligible, which we believe is not obvious, one has to remember that the findings of Vix and Lami apply to each individual distribution of a pure single-tryptophan residue protein. In the complex biological tissues discussed here, however, the expected lifetime distribution should be given by the sum of the distributions of a range of fluorophores and so should be rather broader.

Most previous investigations of the autofluorescence of tissue have used excitation wavelengths in the UV (e.g., Zeng et al., 1993), for which the major fluorophores are tryptophan and NADH, although there is also fluorescence observed from elastin and collagen (Baraga et al., 1991). Work done with longer-wavelength UV excitation has shown that, for excitation at 310/312 nm, the effect of the fluorescence of tryptophan is minimized (Baraga et al., 1991) and that most of the observed fluorescence is due to elastin and collagen. The rejection of tryptophan will be even greater at the excitation wavelength used in our study (415 nm), and so we attribute most of the fluorescence observed in these experiments to elastin and collagen. Although continuous distributions of lifetimes in proteins have been found so far only for tryptophan (Alcala et al., 1987), our work is consistent with elastin and collagen also exhibiting stretched-exponential fluorescence decay profiles and continuous lifetime distributions. The macromolecular aggregates that make up tissue fibers are formed by cross-linking between individual protein molecules. Such linkages, when excited at 415 nm, are the source of the fluorescence of these materials (Pongor et al., 1984). The cross-linking occurs outside the cell and varies considerably with factors such as age and the local chemical environment. This variation could be the origin of the broadening of discrete lifetime values in a molecular microenvironment that cannot be resolved spatially.

Although the use of the StrEF in this work does not require the determination of the distribution of lifetimes $\rho(\tau)$

(see Eq. 4), once determined, the first moment of this distribution corresponds to the mean lifetime $\langle\tau\rangle$ given in Eq. 8. Other moments of the distribution could be of interest as alternative plotting parameters, potentially providing additional contrast in FLIM maps as already done by the heterogeneity parameter. A reliable algorithm to obtain $\rho(\tau)$ has proven to be the CONTIN program (Provencher, 1982), and we envisage in the near future implementing the corresponding algorithm in FLIM analysis.

Due to the equivalence between the time-domain and frequency-domain FLIM, it is expected that the stretched-exponential model can also give substantial improvement to frequency-domain analysis. However, there is no analytical expression for its Fourier transform because of the unusual mathematical behavior of the stretched-exponential function. Numerical approximations to the frequency-domain description of the stretched-exponential model have had limited success due to problems originating from cutoff effects. However, a close relationship has been found between the stretched exponential in the time domain and the Havriliak-Negami function (HNF) in the frequency domain. The exact relationship between both functions has been studied and tested for relaxation experiments by Alvarez et al. (1991) who found a simple relation between the parameters of both functions. The authors concluded that this simple relation is expected to hold for all data that can be described either by the StrEF or the HNF. We think that verification of this prediction would be important because the HNF could provide a potentially useful tool for the frequency-domain FLIM community, complementing the application of the StrEF in the time domain.

From a computational point of view, the stretched-exponential model is highly economical because fewer parameters are needed compared with double- or multi-exponential decay models. This results in significantly faster image processing of FLIM data. It was observed that the time necessary for processing images using the stretched-exponential model was significantly less than that for the double-exponential model, even though both yielded similar goodness of fit. As a comparison, for the FLIM maps of the rat's ear image (Fig. 5) the double-exponential fit took ~1.5 times more processing time than the stretched-exponential fit to the same data. This was mainly caused by the larger amount of computational iterations necessary for the double-exponential model (6,447,720 iterations) as compared with the stretched-exponential model (2,585,025 iterations). This difference in processing speed will be even more pronounced between the stretched-exponential model and higher-multiple-exponential models. For instance, fitting Fig. 5 to a triple-exponential model (not shown) took ~11 times more processing time than the stretched-exponential fit.

A further advantage of the stretched-exponential model is that it describes fluorescence data without the need for making assumptions about the decay (e.g., number of discrete exponential components in a multiple-exponential model), thus making it suitable for fitting fluorescence data with unknown decay characteristics. Even for the analyses of samples other than tissue, the StrEF may be more suitable than conventional multiple-exponential models. As shown in Fig. 1, the deviation of the StrEF from an ideal fit to purely multi-exponential data is very small when the data shows one dominant component, which is a more realistic case than equally strong components. This, together with the fact that fluorophores often interact and/or are located in a wide range of microenvironmental conditions, suggests that the StrEF could be usefully applied in many of these cases. It could then provide important information about the interaction mechanisms broadening the lifetimes. One example might be the widely studied enhanced green fluorescent protein (EGFP), having a dominant ($\alpha_1 = 0.74$) long lifetime component and two other weak ($\alpha_2 = 0.12$, $\alpha_3 = 0.14$) short components (Uskova et al., 2000). The use of the StrEF in this case would also speed up considerably the calculation time compared with a triple-exponential fit (~11 times, as mentioned in the paragraph above), which becomes especially important when lifetime imaging of living cells is attempted.

CONCLUSION

Fluorescence lifetime measurements are potentially non-invasive and allow both the identification of specific fluorophores and the quantitative monitoring of their local environment for biomedical imaging. We have demonstrated that the stretched-exponential model can represent the observed autofluorescence decay profiles in biological tissue very accurately, yielding excellent contrast and spatial image quality for time-domain FLIM maps. This observation is in agreement with earlier suggestions that the complexities in decay mechanisms for fluorescence of tissue proteins such as tryptophan lead to continuous distributions of lifetimes rather than a few discrete lifetime components, and so the StrEF is therefore more realistic than a single- or double-exponential decay model. Due to the relatively long excitation wavelength used in our experiments, the main tissue fluorophores excited are elastin and collagen, rather than tryptophan, but our results suggest that elastin and collagen also exhibit continuous lifetime distributions well represented by a stretched-exponential decay function. The use of such a single generalized decay model also minimizes the processing time and eliminates the need for any presumptive choices on the number of exponential terms currently made when using multiple-exponential models. This is especially useful in non-invasive biomedical imaging that utilizes the autofluorescence of endogenous fluorophores in tissues, because no a priori knowledge of the decay characteristics is required. Besides the mean lifetime $\langle\tau\rangle$ of the continuous lifetime distribution, the stretched-exponential model provides the additional param-

eter h, which is a direct measure for the local heterogeneity of the sample. This heterogeneity parameter should permit the study of mechanisms that broaden the lifetime distributions in complex samples, and it also provides an additional means to contrast different biological components.

We thank Jonathan Jones from the Oxford Center for Quantum Computation for his suggestion to apply the stretched-exponential function to FLIM. We also thank Klaus Suhling from the Chemistry Department at Imperial College and Fernando Alvarez from the University in San Sebastian, Spain, for helpful comments.

This research was funded by the UK Engineering and Physical Sciences Research Council (EPSRC) and the Biotechnology and Biological Sciences Research Council (BBSRC). K.C.B.L. acknowledges a scholarship awarded by the Public Service Commission (Singapore); M.J.C. and K.D. acknowledge EPSRC CASE studentships with the Institute of Cancer Research at the ICR/Royal Marsden National Hospital trust, and S.E.D.W. acknowledges an EPSRC studentship. Finally, we wish to thank our referees for their constructive and informative comments.

REFERENCES

Alcala, J. R. 1994. The effect of harmonic conformational trajectories on protein fluorescence and lifetime distributions. *J. Chem. Phys.* 101: 4578–4584.

Alcala, J. R., E. Gratton, and F. G. Prendergast. 1987. Fluorescence lifetime distributions in proteins. *Biophys. J.* 51:597–604.

Alvarez, F., A. Alegría, and J. Colmenero. 1991. Relationship between the time-domain Kohlrausch-Williams-Watts and frequency-domain Havriliak-Negami relaxation functions. *Phys. Rev. B.* 44:7306–7312.

Bambot, S. B., G. Rao, M. Romauld, G. M. Carter, J. Sipior, E. Terpetchnig, and J. R. Lakowicz. 1995. Sensing oxygen through skin using a red diode laser and fluorescence lifetimes. *Biosensors Bioelectron.* 10: 643–652.

Baraga, J. J., R. P. Rava, M. Fitzmaurice, L. T. Tong, P. Taroni, C. Kittrell, and M. S. Field. 1991. Characterisation of the fluorescent morphological structures in human arterial wall using ultra-violet excited multispectrofluorimetry. *Atherosclerosis.* 88:1–14.

Bevington, P. R. 1969. Data Reduction and Error Analysis for the Physical Sciences. McGraw-Hill, New York.

Clegg, R. M., and P. C. Schneider. 1996. Fluorescence lifetime-resolved imaging microscopy: a general description of lifetime-resolved imaging measurements. *In* Fluorescence Microscopy and Fluorescent Probes. Plenum Press, New York.15–25.

Dowling, K., M. J. Dayel, S. C. W. Hyde, P. M. W. French, M. J. Lever, J. D. Hares, and A. K. L. Dymoke-Bradshaw. 1999. High resolution time-domain fluorescence lifetime imaging for biomedical applications. *J. Mod. Opt.* 46:199–209.

Dowling, K., M. J. Dayel, M. J. Lever, P. M. W. French, J. D. Hares, and A. K. L. Dymoke-Bradshaw. 1998. Fluorescence lifetime imaging with picosecond resolution for biomedical applications. *Opt. Lett.* 23: 810–812.

Förster, T. 1948. Zwischenmolekulare Energiewanderung und Fluoreszenz. *Ann. Phys. (Leipzig).* 2:55–75.

Ghiggino, K. P., and T. A. Smith. 1993. Dynamics of energy migration and trapping in photoirradiated polymers. *Prog. React. Kinet.* 18:375–436.

James, D. R., and W. R. Ware. 1985. A fallacy in the interpretation of fluorescence decay parameters. *Chem. Phys. Lett.* 120:455–459.

Jones, R., K. Dowling, M. J. Cole, D. Parsons-Karavassilis, M. J. Lever, P. M. W. French, J. D. Hares, and A. K. L. Dymoke-Bradshaw. 1999. Fluorescence lifetime imaging using a diode-pumped all-solid-state laser system. *Electron. Lett.* 35:256–257.

Laherrère, J., and D. Sornette. 1998. Stretched exponential distribution in nature and economy: "fat tails" with characteristic scales. *Eur. Phys. J. B.* 2:525–539.

Lakowicz, J. R. 1999. Principles of Fluorescence Spectroscopy, 2nd ed. Kluwer Academic/Plenum Publishers, New York.

Lakowicz, J. R., H. Szmacinski, and K. Nowaczyk. 1992. Fluorescence lifetime imaging. *Anal. Biochem.* 202:316–330.

Maliwal, B. P., J. Kuœba, and J. R. Lakowicz. 1994. Fluorescence energy transfer in one dimension: frequency-domain fluorescence study of DNA-fluorophore complexes. *Biopolymers.* 35:245–255.

Phillips, J. C. 1996. Stretched exponential relaxation in molecular and electronic glasses. *Rep. Prog. Phys.* 59:1133–1207.

Pongor, S., P. C. Ulrich, F. A. Bencsath, and A. Cerami. 1984. Aging of proteins: isolation and identification of a fluorescent chromophore from the reaction of polypeptides with glucose. *Proc. Natl. Acad. Sci. U.S.A.* 81:2684–2688.

Provencher, S. W. 1982. CONTIN: a general purpose constrained regularization program for inverting noisy linear algebraic and integral equations. *Comput. Phys. Commun.* 27:229–242.

Sanders, R., A. Draaijer, H. C. Gerritsen, P. M. Houpt, and Y. K. Levine. 1995. Quantitative pH imaging in cells using confocal fluorescence lifetime imaging microscopy. *Anal. Biochem.* 227:302–308.

Szmacinski, H., and J. R. Lakowicz. 1993. Optical measurements of pH using fluorescence lifetimes and phase-modulation fluorometry. *Anal. Chem.* 13:1668–1674.

Uskova, M., J. Borst, M. Hink, A. van Hoeck, A. Schots, N. Klyachko, and A. Visser. 2000. Fluorescence dynamics of green fluorescent protein in AOT micelles. *Biophys. Chem.* 87:73–84.

Vix, A., and H. Lami. 1995. Protein fluorescence decay: discrete components or distribution of lifetimes? Really no way out of the dilemma? *Biophys. J.* 68:1145–1151.

Zeng, H., C. Mac Aulay, B. Palcic, and D. I. McLean. 1993. A computerised autofluorescence and diffuse reflectance spectroanalyser system for in vivo skin studies. *Phys. Biol. Med.* 38:231–240.